Metadata of the article that will be visualized in OnlineFirst

ArticleTitle	Prospects of a tether system deployed at the L1 libration point	
Article Sub-Title		
Article CopyRight	The Author(s), under exclusive licence to Springer Nature B.V. (This will be the copyright line in the final PDF)	
Journal Name	Nonlinear Dynamics	
Corresponding Author	Family Name	**Aslanov**
	Particle	
	Given Name	**Vladimir S.**
	Suffix	
	Division	
	Organization	Samara National Research University
	Address	34, Moscovskoe shosse, Samara, Russia, 443086
	Phone	
	Fax	
	Email	aslanov_vs@mail.ru
	URL	http://aslanov.ssau.ru/
	ORCID	http://orcid.org/0000-0003-4065-137X
Schedule	Received	5 April 2021
	Revised	
	Accepted	2 September 2021

Abstract

The paper focuses on the study and development of a mission to use the L1 libration point for deployment of a tether system in the direction of a moon in the planar elliptic restricted three-body problem on the example of the Mars-Phobos system. An orbiting spacecraft, which deploys the tether system, is located at the L1 libration point and is held at this point by the low thrust of its engines. The classical equations in the Nechville variables are converted into equations in polar coordinates and, for the particular case when the tether is inextensible and two primaries moving in circular orbits about their mass center. These equations are integrated in quadrature, and the equilibrium positions and the oscillation period of the tether are found. As a result of eccentricity, the primaries move on ellipses around the barycenter, which rotates with angular velocity equal to that of the primaries, the position of the two-body pulsates along the axis connecting them. A new mission architecture is proposed, which includes three successive stages: initial deployment to the upper pulsation point (perigee), angular stabilization of the tether relative to the lower stable position, and maintaining a constant distance to a moon's surface. An end mass with measuring equipment of this tether system can be set directly on the moon's surface. Numerical simulations have shown the effectiveness of the proposed control laws of the tether system at all stages of the mission for the Mars-Phobos system, in which the L1 libration point is located quite close to the Phobos' surface (~ 3.4 km). This paper is the first effort, using to justify publicly the possibility of implementing a mission with a tether system "attached" at L1 libration point to study surface of moons based on the proposed control laws and the sequence of their application. The results of this study can be used to enable many future missions throughout the solar system. If in the future similar missions will be approved, then undoubtedly more advanced control methods of this kind of systems will be developed.

Keywords (separated by '-')	L1 libration point - Tether system - Stability and instability - Exact solutions - Control laws
Footnote Information	

Nonlinear Dyn
https://doi.org/10.1007/s11071-021-06884-4

ORIGINAL PAPER

Prospects of a tether system deployed at the L1 libration point

Vladimir S. Aslanov

Received: 5 April 2021 / Accepted: 2 September 2021

Abstract The paper focuses on the study and development of a mission to use the L1 libration point for deployment of a tether system in the direction of a moon in the planar elliptic restricted three-body problem on the example of the Mars-Phobos system. An orbiting spacecraft, which deploys the tether system, is located at the L1 libration point and is held at this point by the low thrust of its engines. The classical equations in the Nechville variables are converted into equations in polar coordinates and, for the particular case when the tether is inextensible and two primaries moving in circular orbits about their mass center. These equations are integrated in quadrature, and the equilibrium positions and the oscillation period of the tether are found. As a result of eccentricity, the primaries move on ellipses around the barycenter, which rotates with angular velocity equal to that of the primaries, the position of the two-body pulsates along the axis connecting them. A new mission architecture is proposed, which includes three successive stages: initial deployment to the upper pulsation point (perigee), angular stabilization of the tether relative to the lower stable position, and maintaining a constant distance to a moon's surface. An end mass with measuring equipment of this tether system can be set directly on the moon's surface. Numerical simulations have shown the effectiveness of the proposed control laws of the tether system at all stages of the mission for the Mars-Phobos system, in which the L1 libration point is located quite close to the Phobos' surface ($\sim$ 3.4 km). This paper is the first effort, using to justify publicly the possibility of implementing a mission with a tether system "attached" at L1 libration point to study surface of moons based on the proposed control laws and the sequence of their application. The results of this study can be used to enable many future missions throughout the solar system. If in the future similar missions will be approved, then undoubtedly more advanced control methods of this kind of systems will be developed.

Keywords L1 libration point · Tether system · Stability and instability · Exact solutions · Control laws

1 Introduction

The field of space tethers has received very much attention in recent decades, with several books [1–4] and many papers (eg. [5–18]) available in the scientific literature. The fundamental book by Beletsky and Levin [1] has played an important role in providing the basis for the study of the space tethered system

V. S. Aslanov (✉)
Samara National Research University, 34, Moscovskoe shosse, Samara, Russia 443086
e-mail: aslanov_vs@mail.ru
URL: http://aslanov.ssau.ru/

dynamics. The advent of space tether systems starts a new era in space research. The tether systems can emerge as a new technology for developing the planets of the solar system, their moons [16], and the exploitation of other celestial bodies, as well as asteroids [14]. In cases of the study of the tether dynamics in the gravitational fields of two bodies, one cannot do without considering the three-body problem, as for example [16]. The restricted three-body problem is the foundation for solving many applied problems of astronautics, in particular, for the computation of interplanetary flights. A detailed analysis of main studies on this topic can be found in the Szebehely's textbook [19], which discusses a variety of motion states, equilibrium positions, motion near these positions, application of Hamiltonian dynamics methods to the restricted problem, its periodic orbits, and other aspects. Currently, a large number of papers on the restricted three-body problem have been published (e.g., [20–25]), in which this problem is studied in detail, and these results are widely used in various astronautical missions. It should be pointed out here that the above references are not an exhaustive analysis of the literature on the topic in question, which is very extensive and includes a huge number of works, but they do provide some insight into the AQ2 problem.

In 2017, NASA proposed an innovative mission architecture to explore the surface of Phobos utilizing a tether system "anchored" at the L1 libration point [16]. As a release point of the tether, it was proposed to use an orbiting spacecraft, which should hover in the vicinity of the L1 libration point of the Mars-Phobos system. This mission was called Phobos L1 Operational Tether Experiment (PHLOTE). Kempton, Pearson, Levin, Carroll, and Amzajerdian have investigated the key technical challenges associated with implementing the PHLOTE mission at the Mars-Phobos L1 libration point location. PHLOTE deployment dynamics has been simulated in the first approximation, and a set of suitable deployment trajectories has been identified. After deployment, the tether reel control damps residual longitudinal and lateral oscillations by periodically reeling a short segment of the tether in and out, based on the measurements of some parameters. However, the stabilization effect is achieved in a very particular region in the parameter space. This PHLOTE initial study provides a compelling example that many future missions throughout the solar system can use. Obviously, the new engineering ideas require solutions of new fundamental problems. The PHLOTE report [16] has provided many of the hardware solutions, technical details needed to implement the mission. Nevertheless, such a complex innovative mission requires an additional theoretical substantiation and a possible multiplicity of analytical models of the system motion and control laws of the tether system.

The paper focuses on the study and development of a mission similar to the PHLOTE mission, in which the L1 libration point is used to deploy the tether system in the direction of the moon. An orbiting spacecraft, further referred to simply as the orbiter, which deploys the tether system, is located at the L1 libration point and is held at this point by the low thrust of its engines. The goal of the paper is to study the behavior of the system and develop control of the deployment and stabilization of the tether system at a certain distance from a moon's surface of the L1-moon mission. The proposed mission includes three successive stages: initial deployment from the L1 libration point to the upper pulsation point (perigee), angular stabilization of the tether relative to the lower stable position, and maintaining a constant distance to the moon's surface. The last stage is related to an eccentricity, since due to it the primaries move on ellipses around the barycenter, which rotates with angular velocity equal to that of the primaries, the position of the two-body pulsates along the axis connecting them. This paper is not directed at developing control algorithms for similar tether systems in detail. It is the first effort, using to justify publicly the possibility of implementing a mission with a tether system "attached" at the L1 libration point to study surface of moons. It is based on the proposed control laws and the sequence of their application.

Initially, in terms of the planar restricted three-body problem, the motion equations are written in the rotating Cartesian coordinate system in Nechville variables and these equations are then converted to dimensionless equations in polar coordinates relative to the L1 libration point. Next, for the particular case when the tether is inextensible and the primaries move on circular paths around the barycenter of the system, these equations are integrated in quadrature, the equilibrium positions and the oscillation period of the tether are found. The proposed control laws of the

Journal : Medium 11071 | Dispatch : 9-9-2021 | Pages : 13
Article No. : 6884 | LE | TYPESET
MS Code : NODY-D-21-00862R1 | CP | DISK

tether system at the first stage provide the initial (basic) deployment, at the second stage ensures stabilization of the tether relative to the lower stable position of equilibrium closest to the moon's surface, and the last stage realizes control of deployment and retrieval of the tether due to pulsating motions of the L1 libration point caused by the eccentricity of the primaries orbits. As an example, the Mars-Phobos system is considered, in which the L1 libration point is located quite close to the Phobos' surface ($\sim$ 3.4 km). And if necessary, a measuring equipment can be set on end mass of this tether system directly on the moon's surface. The numerical simulations have shown the effectiveness of the proposed control laws of the tether system at all stages of the mission for the Mars-Phobos system. And finally, conclusions about the feasibility of the implementation of the suggested mission and features of the behavior of the tether system using the proposed control laws are made.

2 Dimensionless equations of motion in polar coordinates relative to L1 libration point

In this section, we derive the planar motion equations of a small body M in two gravitational fields of two primaries M_1 and M_2 (Planet-Moon) in polar coordinates relative to the L_1 libration point in terms of the classical elliptic three-body problem [19, 26]. It is assumed that the mass of the body M is many times less than the mass of the bodies M_1 and M_2. Therefore, the body M has negligible effect on the other bodies. It is also supposed that the bodies M_1 and M_2 move in elliptical orbits around their mutual mass center. The distance between the two primaries is

$$r = \frac{p}{1 + e\cos f} \tag{1}$$

where p is the semilatus rectum, e is the eccentricity of the two-body orbit of the primaries, and f is the true anomaly. The orbiter is located at the L1 libration point, which is the attachment point for the tether system, as it will be discussed further. In the barycentre-centered synodic coordinate system, which rotates with the two primaries and using Nechvile's variables (ξ, η), the small body's motion can be described in dimensionless form as [19, 26]

$$\xi'' - 2\eta' = \frac{1}{1 + e\cos f}\frac{\partial\Omega}{\partial\xi} \tag{2}$$

$$\eta'' + 2\xi' = \frac{1}{1 + e\cos f}\frac{\partial\Omega}{\partial\eta} \tag{3}$$

where Ω is the potential function given by

$$\Omega = \frac{1}{2}\left(\xi^2 + \eta^2\right) + \frac{1-\mu}{r_1} + \frac{\mu}{r_2} \quad \left(0 < \mu \leq \frac{1}{2}\right) \tag{4}$$

$$r_1 = \sqrt{(\xi + \mu)^2 + \eta^2} \quad r_2 = \sqrt{(\xi + \mu - 1)^2 + \eta^2} \tag{5}$$

where $(.)' = \frac{\mathrm{d}}{\mathrm{d}f}(.)$ and $(.)'' = \frac{\mathrm{d}^2}{\mathrm{d}f^2}(.)$; $\mu = \frac{m_2}{m_1 + m_2}$ is the mass ratio; m_1 and m_2 are masses of the bodies M_1 and M_2, respectively.

The coordinates ξ for the collinear libration points (L_1, L_2 and L_3) can be determined in terms of the mass ratio μ as the roots of the following equation [26]

$$\xi - \mu\frac{|\mu + \xi - 1|}{(\mu + \xi - 1)^3} - (1-\mu)\frac{|\mu + \xi|}{(\mu + \xi)^3} = 0 \tag{6}$$

Next, to determine the coordinate of the L_1 libration point, we use the well-known approximate formula. It is possible to find a more exact formula, but this does not change the essence, since this coordinate depends only on the unchanging mass ratio μ

$$\xi_1 = 1 - \left(\frac{\mu}{3}\right)^{1/3} = \sigma \tag{7}$$

Position of the body M relative to the L_1 libration points in a polar reference frame (l, α) is defined by substituting the variables

$$\xi = \sigma + lk\cos\alpha, \quad \eta = lk\sin\alpha \tag{8}$$

where $k = 1 + e\cos f$, $l = \frac{L}{p}$ is the dimensionless distance, L is the distance between the small body and the L1 libration point, or in this case, tether length.

Eqs. motion (2) and (3) in the polar reference frame (Fig. 1) are written as

$$\alpha'' + F_\alpha = 0 \tag{9}$$

Journal : Medium 11071 | Dispatch : 9-9-2021 | Pages : 13
Article No. : 6884 | LE | TYPESET
MS Code : NODY-D-21-00862R1 | CP | DISK

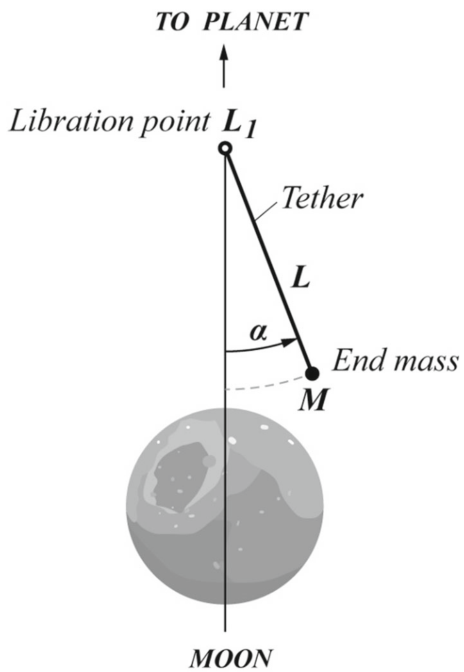

Fig. 1 The polar frame (L, α)

$$l'' + F_l = 0 \tag{10}$$

where

$$F_\alpha = -\left[\frac{2(1+\alpha')(el\sin f - kl')}{lk} - \frac{\sigma\sin\alpha}{lk^2} + \frac{\mu(\mu-1+\sigma)\sin\alpha}{lk^2\left((\mu-1+\sigma)^2 + kl(2(\mu-1+\sigma)\cos\alpha + kl)\right)^{3/2}} - \frac{(-1+\mu)(\mu+\sigma)\sin\alpha}{lk^2\left((\mu+\sigma)^2 + kl(2(\mu+\sigma)\cos\alpha + kl)\right)^{3/2}}\right] \tag{11}$$

$$F_l = -\left[\frac{2el'\sin f}{k} + (1+\alpha')^2 l + \frac{\sigma\cos\alpha}{k^2} - \frac{\mu((\mu-1+\sigma)\cos\alpha + kl)}{k^2\left((\mu-1+\sigma)^2 + kl(2(\mu-1+\sigma)\cos\alpha + kl)\right)^{3/2}} + \frac{(-1+\mu)((\mu+\sigma)\cos\alpha + kl)}{k^2\left((\mu+\sigma)^2 + kl(2(\mu+\sigma)\cos\alpha + kl)\right)^{3/2}}\right] \tag{12}$$

3 Constant-length tether

A better understanding of the tether motion in the two-body gravitational field in terms of the restricted three-body problem can be achieved by considering the simple case when a weightless and inextensible tether with an end body is attached to the L_1 libration point. In this case, Eq. (9) describes the oscillation of a material point on an inextensible tether

$$L = \text{const} \rightarrow l = \text{const} \tag{13}$$

This helps to determine equilibrium positions, to find a period of oscillations and to identify some other regularities of motion of a peculiar pendulum in the two-body gravitational field. If condition (13) is satisfied, the motion of the end body M is described by only one differential equation (9) as follows

$$\alpha'' = \frac{2e(1+\alpha')\sin f}{k} - \frac{\sigma\sin\alpha}{k^2 l} + \frac{\mu(\mu-1+\sigma)\sin\alpha}{k^2 l\left((\mu-1+\sigma)^2 + kl(2(\mu-1+\sigma)\cos\alpha + kl)\right)^{3/2}} - \frac{(-1+\mu)(\mu+\sigma)\sin\alpha}{k^2 l\left((\mu+\sigma)^2 + kl(2(\mu+\sigma)\cos\alpha + kl)\right)^{3/2}} \tag{14}$$

If two primaries move in circular orbits ($e = 0$, $k = 1 + e\cos f = 1$), then Eq. (14) takes the form

$$\alpha'' + F(\alpha) = 0 \tag{15}$$

where the dimensionless generalized force is written as

$$F(\alpha) = \frac{\sigma\sin\alpha}{l} - \frac{\mu(\mu-1+\sigma)\sin\alpha}{l\left((\mu-1+\sigma)^2 + l(2(\mu-1+\sigma)\cos\alpha + l)\right)^{3/2}} - \frac{(1-\mu)(\mu+\sigma)\sin\alpha}{l\left((\mu+\sigma)^2 + l(2(\mu+\sigma)\cos\alpha + l)\right)^{3/2}} \tag{16}$$

This equation has the following energy integral

$$\frac{(\alpha')^2}{2} + W(\alpha) = E \tag{17}$$

where E is the total energy, the potential energy is written as

Journal : Medium 11071 | Dispatch : 9-9-2021 | Pages : 13
Article No. : 6884 | ☐ LE | ☐ TYPESET
MS Code : NODY-D-21-00862R1 | ☑ CP | ☑ DISK

$$W(\alpha)=\int F(\alpha)\mathrm{d}\alpha = -\frac{\sigma\cos\alpha}{l}-\frac{\mu}{l^2\sqrt{l^2+(\mu-1+\sigma)^2+2l(\mu-1+\sigma)\cos\alpha}} - \frac{1-\mu}{l^2\sqrt{l^2+(\mu+\sigma)^2+2l(\mu+\sigma)\cos\alpha}} \tag{18}$$

Figure 2 shows the generalized force (16), the potential energy (18), and the corresponding phase portrait of the system (15).

Equating Eq. (16) to zero

$$F(\alpha_*)=0 \tag{19}$$

leads to two types of stationary positions for $\alpha\in[-\pi,\pi]$. The stable equilibrium positions are $\alpha_s=-\pi,0,\pi$, and the unstable positions in the vicinity of the points are $\alpha_{us}=\frac{\pi}{2}$ and $\alpha_{us}=-\frac{\pi}{2}$. At the points of the stable and unstable equilibrium positions, the following conditions

$$\left.\frac{\partial F}{\partial\alpha}\right|_{\alpha=\alpha_s}=\left.\frac{\partial^2 W}{\partial\alpha^2}\right|_{\alpha=\alpha_s}>0,\quad \left.\frac{\partial F}{\partial\alpha}\right|_{\alpha=\alpha_{us}}=\left.\frac{\partial^2 W}{\partial\alpha^2}\right|_{\alpha=\alpha_{us}}<0 \tag{20}$$

are satisfied as shown in Fig. 2. Differentiating Eq. (16), we have

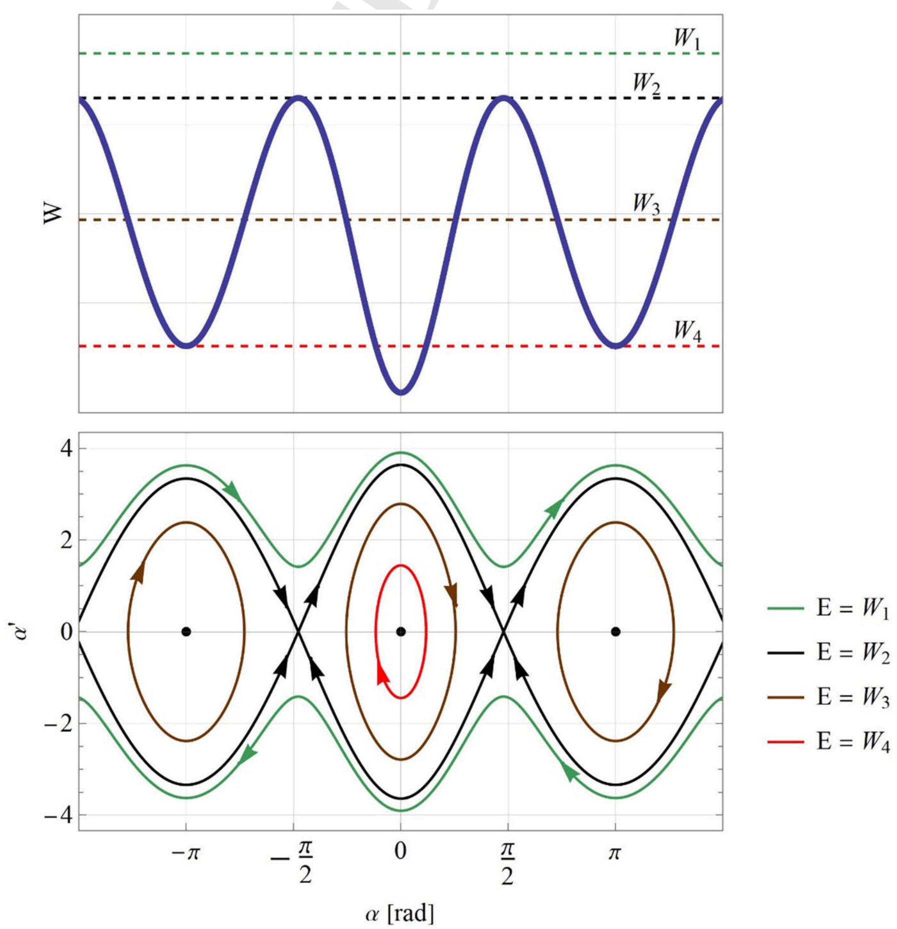

Fig. 2 Representations of **a** the potential energy $W(\alpha)$, **b** the separatrices $\alpha'(\alpha)$ in the phase space corresponding to different levels of the total energy W_i $(i=1,2,3,4)$ for the tether length $L=pl=3000\,\mathrm{m}$

Journal : **Medium 11071**	Dispatch : **9-9-2021**	Pages : **13**
Article No. : **6884**	□ LE	□ TYPESET
MS Code : **NODY-D-21-00862R1**	✔ CP	✔ DISK

$$\frac{\partial F}{\partial \alpha}=\frac{\cos\alpha}{l}\left[\sigma-\frac{\mu(\mu-1+\sigma)}{\left(l^2+2l(\mu-1+\sigma)\cos\alpha+(\mu-1+\sigma)^2\right)^{3/2}}+\frac{(\mu-1)(\mu+\sigma)}{\left(l^2+2l(\mu+\sigma)\cos\alpha+(\mu+\sigma)^2\right)^{3/2}}\right]-3\sin^2\alpha\left[\frac{\mu(\mu-1+\sigma)}{\left(l^2+2l(\mu-1+\sigma)\cos\alpha+(\mu-1+\sigma)^2\right)^{5/2}}-\frac{(\mu-1)(\mu+\sigma)}{\left(l^2+2l(\mu+\sigma)\cos\alpha+(\mu+\sigma)^2\right)^{5/2}}\right]$$

Using Eqs. (17) and (18), one can find the period of oscillations of the tether by the true anomaly f relative to the stable equilibrium position $\alpha_s=0$. The initial condition takes the following

$$f=0:\quad \alpha_0=\alpha_m,\ \alpha_0'=0 \tag{21}$$

where α_m is the oscillation amplitude. According to Eq. (17) and the conditions (21), the total energy is defined as

$$E=W(\alpha_m) \tag{22}$$

Obviously, the tether oscillation occurs between symmetrical extreme positions of the tether $\alpha\in[-\alpha_m,\alpha_m]$. According to (17), the oscillation period is determined by the equation

$$P=\int_0^P \mathrm{d}f=2\int_{-\alpha_m}^{\alpha_m}\frac{\mathrm{d}\alpha}{\sqrt{2[W(\alpha_m)-W(\alpha)]}} \tag{23}$$

As follows from Eqs. (23) and (18), the oscillation period P depends on the oscillation amplitude α_m and the dimensionless tether length l. If the tether oscillates relative to the position of stable equilibrium $\alpha_s=\pi$, then the oscillation period is written as

$$P=\int_0^P \mathrm{d}f=2\int_{\pi-\alpha_m}^{\pi+\alpha_m}\frac{\mathrm{d}\alpha}{\sqrt{2[W(\pi+\alpha_m)-W(\alpha)]}} \tag{24}$$

To approximate the oscillation frequency of a constant-length tether, Eq. (15) is given in a linearized form ($\sin\alpha\approx\alpha,\ \cos\alpha\approx 1$)

$$\alpha''+\omega^2\alpha=0 \tag{25}$$

where

$$\omega^2=\frac{\sigma}{l}-\frac{\mu(\mu-1+\sigma)\sin\alpha}{l\left((\mu-1+\sigma)^2+l(2(\mu-1+\sigma)+l)\right)^{3/2}}-\frac{(1-\mu)(\mu+\sigma)}{l\left((\mu+\sigma)^2+l(2(\mu+\sigma)+l)\right)^{3/2}}$$

Assuming that the length of the tether is much smaller than the distance between the primaries ($l=\frac{L}{p}\ll 1$), the frequency of oscillation of the tether is written as

$$\omega\approx\sqrt{\frac{d}{L}\left[\sigma+\frac{\mu}{(-1+\mu+\sigma)^2}+\frac{-1+\mu}{(\mu+\sigma)^2}\right]-3\left[\frac{\mu}{(-1+\mu+\sigma)^3}+\frac{-1+\mu}{(\mu+\sigma)^3}\right]+6\frac{L}{d}\left[\frac{\mu}{(-1+\mu+\sigma)^4}+\frac{-1+\mu}{(\mu+\sigma)^4}\right]} \tag{26}$$

Figure 3 shows that in gravitational fields of two heavy bodies in a rotating frame, the oscillation frequency of the pendulum "attached" to the point L1

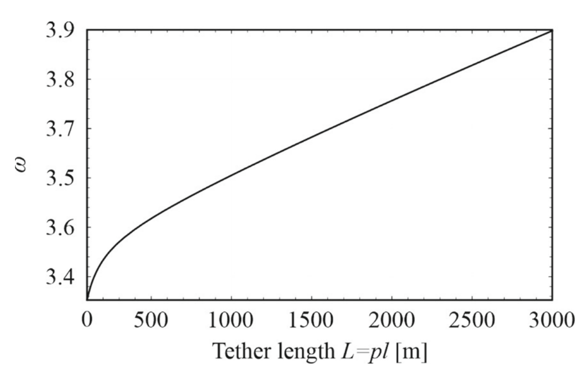

Fig. 3 Oscillation frequency (26) as a function the tether length L for the L1 libration point of the Mars-Phobos system

Journal : Medium 11071 | Dispatch : 9-9-2021 | Pages : 13
Article No. : 6884 | LE | TYPESET
MS Code : NODY-D-21-00862R1 | CP | DISK

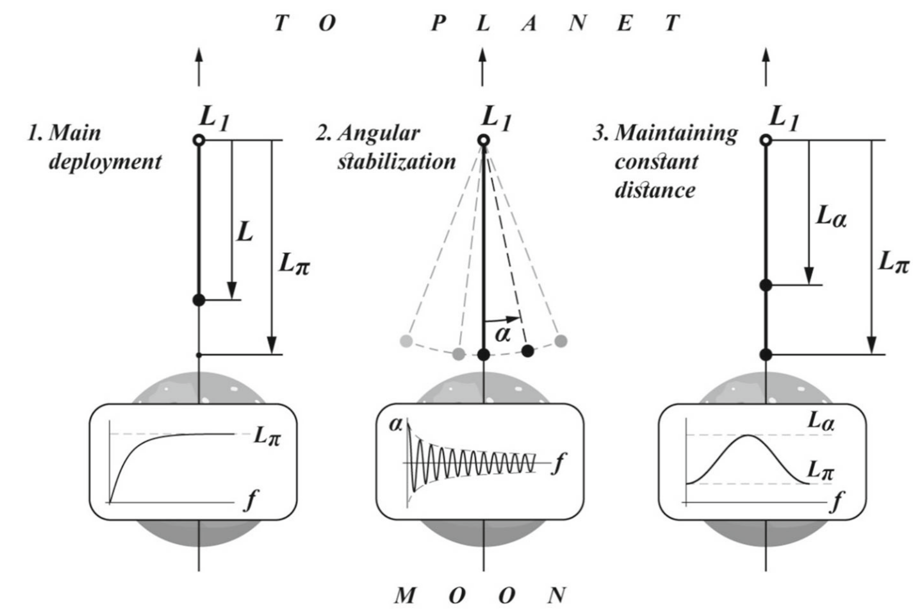

Fig. 4 Three stages of tether deployment

increases with the increase in length, in contrast to classical mathematical pendulum, in which the frequency decreases with the increase in the length of the pendulum ($\sqrt{g/L}$, where g is the gravitational acceleration).

4 Maintaining a constant distance from body M_2

The main objective of this study is to develop a deployment mission of the tether system from the orbiter located at the L1 point to a given distance from the moon's surface, so that the end body M of the tether system is in equilibrium relative to the line (local vertical) connecting the primaries M_1 and M_2. Consider elliptical orbits of the primaries, then due to their eccentricity, the L1 libration point pulsates in the range corresponding to the perigee ($f = 0$) and apogee ($f = \pi$) of their orbits. We propose to divide the whole deployment mission of the tether system into three successive stages (Fig. 4):

1. The initial (basic) deployment of the tether from the L1 point to a given length, which corresponds to the perigee, so that at the end point the deployment rate is equal to zero ($l' = \mathrm{d}l/\mathrm{d}f = 0$).
2. The angular stabilization of the end body relative to the lower stable equilibrium position ($\alpha \to 0$) closest to the moon's surface.
3. The control of deployment and retrieval of the tether to maintain a constant distance to the moon's surface due to pulsations of the L1 libration point.

Now, consider these stages of the deployment of the tether system.

4.1 Basic deployment of the tether

At this stage, the problem about deploying the tether system to a given distance corresponding to perigees of the orbits of the primaries is solved after the ejection of the end mass from the orbiter. The deployment of the tether will be provided by the tension force, therefore, we rewrite the equations of motion (9) and (10) taking into account this force as

$$\alpha'' + F_\alpha = 0 \tag{27}$$

$$l'' + F_l = T \tag{28}$$

where T is a dimensionless tension force.

After separation from the orbiter with an ejection velocity $V_0 = l'_0$, it is necessary to ensure a zero velocity $V_f = l'_f = 0$, when the tether reaches the given length $l = l_f$ at the end point. At this stage, the feedback algorithm (variable linear feedback) is taken as a law of tension of the tether, the effectiveness of

Journal : Medium 11071 | Dispatch : 9-9-2021 | Pages : 13
Article No. : 6884 | ☐ LE | ☐ TYPESET
MS Code : NODY-D-21-00862R1 | ☑ CP | ☑ DISK

which will be demonstrated in the simulation below. And so, the control law can be written as

$$T_1 = k_{1l}\left(l - l_f\right) + k_{1V} l' \tag{29}$$

The dimensionless coefficients k_{1l} and k_{1V} are determined from the satisfaction of the final conditions

$$l = l_f, \; l_f' = 0 \tag{30}$$

4.2 Angular stabilization of the tether

If during the deployment of the tether in the first stage, as a result of the influence of unaccounted disturbances, there are significant oscillations of the tether relative to the lower stable position $\alpha_s = 0$, then stabilization is required to reduce the amplitude of the oscillations before the next stage of deployment of the tether. To generate a control law for the tether tension force, we use the control law ($l = l_f + \lambda\alpha' \sin\alpha$) for a pendulum with a moving mass, which provides, on average, asymptotic stability of the pendulum [27], and write for our case the law of the tether tension force as

$$T_2 = k_{2l}\left[l - \left(l_f + \lambda\alpha' \sin\alpha\right)\right] + k_{2V} l' \tag{31}$$

where k_{2l}, k_{2V}, λ are the control dimensionless coefficients.

4.3 Maintaining a constant distance from moon's surface

The last stage of a deployment-retrieval of the tether is continuous: The distance from the end body attached on the tether to the moon's surface must remain constant. The deployment occurs when the moon moves from perigee to apogee, and the retrieval takes place during the motion of the moon in the opposite direction from apogee to perigee. And so, the tether is attached at the L1 libration point and the primaries move in elliptical orbits. Let us first derive the equation describing the change in length to ensure the constant distance from the end body to the moon's surface. The distance between the primaries M_1 and M_2 is determined by Eq. (1), which corresponds to the Nechville's coordinates

$$\xi = 1, \; \eta = 0 \tag{32}$$

The L_1 point corresponding to Eq. (7) in Nechville's coordinates is defined as

$$\xi_1 = \sigma, \; \eta_1 = 0 \tag{33}$$

Taking into account that L is the dimensional tether length, and d is the dimensional distance from the point M_2 to the point where the end body should be located on the line M_1M_2, the following equation can be written as

$$d + L = r(1 - \sigma) \tag{34}$$

or

$$L = r(1 - \sigma) - \mathrm{d} \tag{35}$$

In dimensionless form, this equation is written as

$$l = \frac{L}{p} = \frac{1 - \sigma}{1 + e\cos f} - \delta \tag{36}$$

where $\delta = \frac{\mathrm{d}}{p}$ is the relative distance from the point M_2 to the end mass. From Eq. (36), it is clear that at the apogee and at the perigee of the primaries orbits, the relative lengths of the tether are, respectively,

$$l_\alpha = \frac{1 - \sigma}{1 - e} - \delta, \; l_\pi = \frac{1 - \sigma}{1 + e} - \delta \tag{37}$$

where l_α, l_π correspond to the apogee and the perigee, respectively.

Using Eq. (36), the tension force control law, which ensures the constant distance from the end body attached on the tether to the primary M_2, can be represented as

$$T_3 = k_{3l}\left[l - \left(\frac{1 - \sigma}{1 + e\cos f} - \delta\right)\right] + k_{3V} l' \tag{38}$$

5 Numerical modeling

This section shows the effectiveness of the proposed control laws at all stages of the tether system deployment on the basis of numerical simulation. In addition, the oscillation period and unstable positions of the constant-length tether fixed at the L1 libration point are numerically determined. As an example, the Mars-Phobos system is considered, in which the L1 libration point is located quite close to the Phobos' surface ($\sim$ 3.4 km). At all stages, the simulation is

Journal : Medium 11071 | Dispatch : 9-9-2021 | Pages : 13
Article No. : 6884 | ☐ LE | ☐ TYPESET
MS Code : NODY-D-21-00862R1 | ☑ CP | ☑ DISK

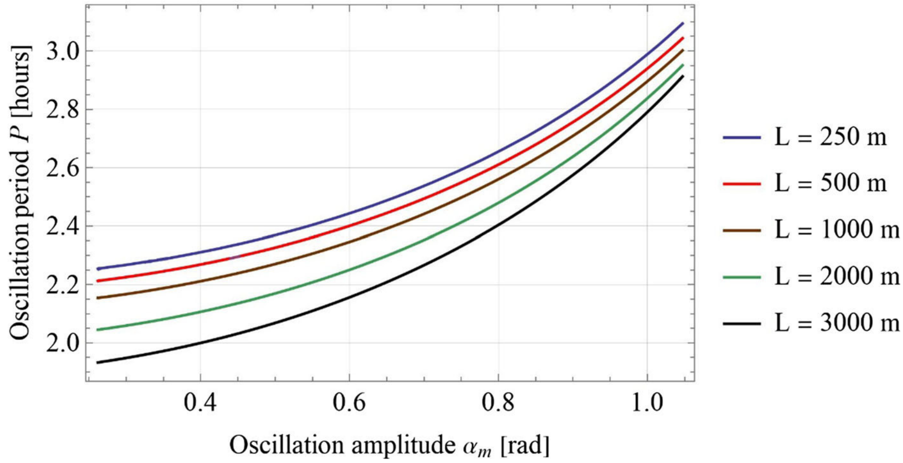

Fig. 5 The oscillation period for the different tether lengths $L = p\,l$

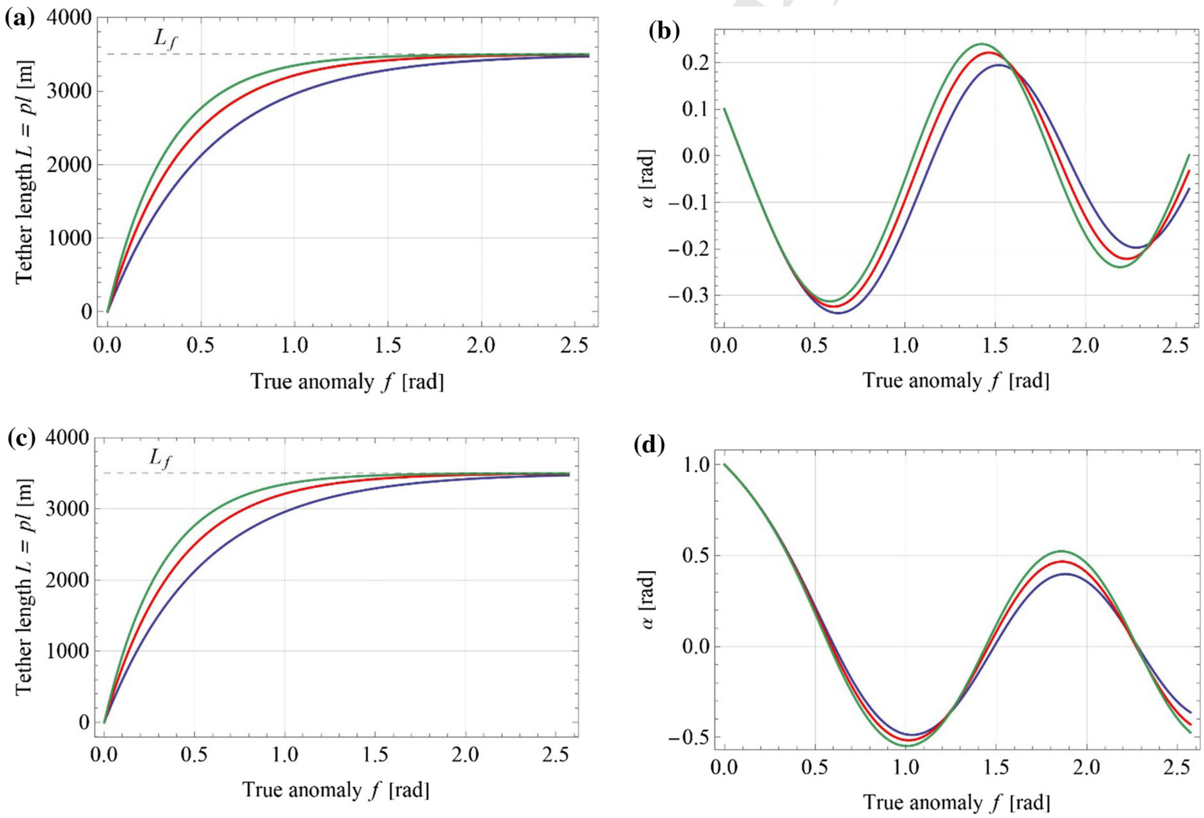

Fig. 6 The tether deployment length and the oscillation angle of the tether for the ejection velocity V_0: 1.5 m/s—blue, 2.0 m/s—red, 2.5 m/s—green

performed by numerical integration of Eqs. (9) and (10).

5.1 Oscillation period of the constant-length tether

Figure 5 depicts the oscillation period of the tether system relative to the lower stable position $\alpha_S = 0$

Journal : Medium 11071 | Dispatch : 9-9-2021 | Pages : 13
Article No. : 6884 | LE | TYPESET
MS Code : NODY-D-21-00862R1 | CP | DISK

depending on the oscillation amplitude α_m of the tether. Observe that the greater the oscillation amplitude of the tether, the greater the oscillation period. So if a relatively short tether ($L = 250$ m) is used and its oscillation amplitude is 1.05 rads, then the period of oscillation is 3.2 h. For a long tether ($L = 3000$ m) and small amplitude (0.26 rads), the period of oscillation is 2.1 h. At the same time, note that, the orbital period of Phobos around Mars is 7.65 h.

5.2 Main deployment of the tether

For this deployment stage, we investigate the influence of two factors: the velocity and direction of the tether ejection from the orbiter, using the Mars-Fobos system as an example. The effectiveness of the control law (29) is illustrated with simulation results on the example of the Mars-Phobos system. A payload (end mass) of the tether system is separated from the orbiter with the ejection velocity V_0: 1.5 m/s, 2.0 m/s, 2.5 m/s. Figure 6a, b corresponds to the initial deflection angle α_0 of the tether equals to 0.1 rad, and Fig. 6c, d to 1.0 rad. The tether system parameters are taken to be payload mass $m = 10$ kg, final tether deployment length $L_f = p\, l_f = 3500$ m, the dimensionless coefficients from Eq. (29) $k_{1l} = -50000$ and $k_{1V} = -16000$. Figure 6b, d shows that the tether is deployed to its full length, while the angular oscillations of the tether are not stabilized. In all three considered cases (Fig. 5), the tether is always stretched, and the tension force of the tether does not exceed 0.7 N.

As shown in Fig. 6, the ejection velocity has little effect on the deployment of the tether. The situation is more complicated with the direction of the ejection velocity, since the tether can be deployed both toward Phobos and toward Mars. The boundaries of these areas for the ejection angle (toward Phobos or toward Mars) are the points of an unstable equilibrium α_{us}. In the case of a circular orbit and a constant tether length, these points are defined as the solution of Eq. (19). In the general case, the unstable equilibrium position α_{us} changes depending on the tether length l, eccentricity e, and true anomaly f. The unstable equilibrium position ($\alpha_{us} = 2.477$ radian) is found by selection with the use of numerical simulation Eqs. (27) and (28) describing the deployment of the tether. In connection with the above, choose the following ejection angles

$$\alpha_0 = 0,\ \frac{\pi}{4},\ \frac{\pi}{2},\ 2.477,\ \frac{3\pi}{4},\ \pi \tag{39}$$

The ejection velocity is assumed to be the same for all cases, equal и $V_0 = L_0' = 2.0$ m/s. Figure 7a demonstrates that the deployment of the tether $L(f)$ does not depend on the ejection angle α_0. As follows from Fig. 7b, to deploy the tether toward Phobos, the ejection angle must belong to the range

$$\alpha_0 \in (-2.477, 2.477) \tag{40}$$

5.3 Angular stabilization of the tether

At the second stage, angular stabilization is realized by means of the control law (31). Two cases of the angular stabilization of the tether are considered:

– the deployment of the tether toward Phobos (Fig. 8), the control coefficient $\lambda = 4 \cdot 10^{-5}$.

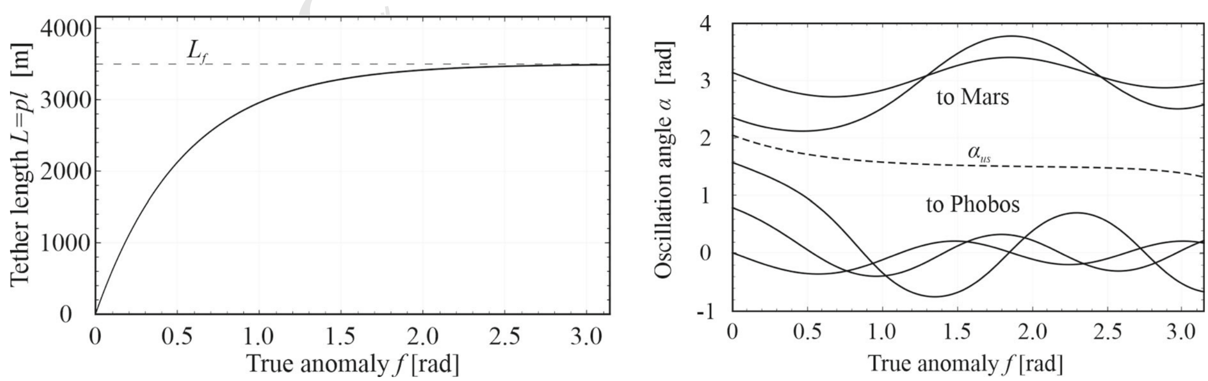

Fig. 7 The tether deployment length and the oscillation angle of the tether for different initial ejection angles (39)

Journal : Medium 11071 Dispatch : 9-9-2021 Pages : 13
Article No. : 6884 LE TYPESET
MS Code : NODY-D-21-00862R1 CP DISK

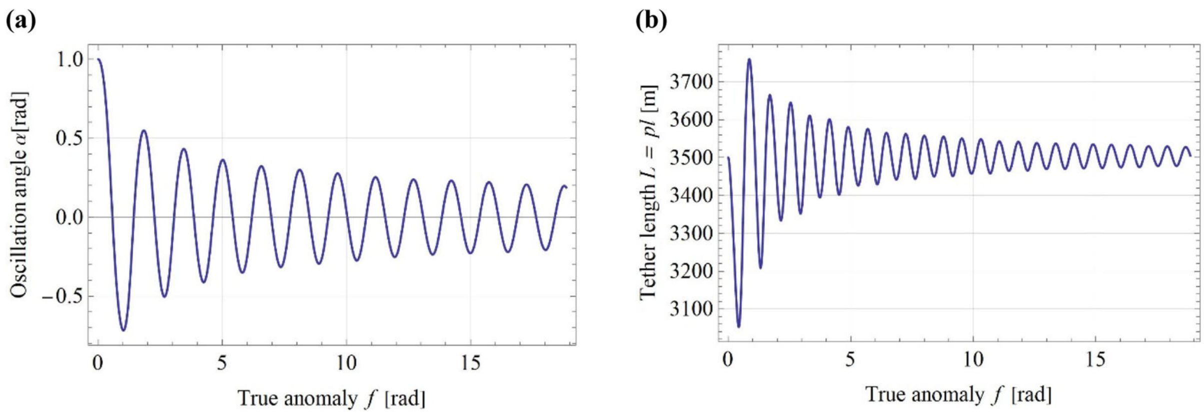

Fig. 8 The deployment of the tether toward Phobos. **a** The oscillation angle α and **b** the tether length $L = p\,l$

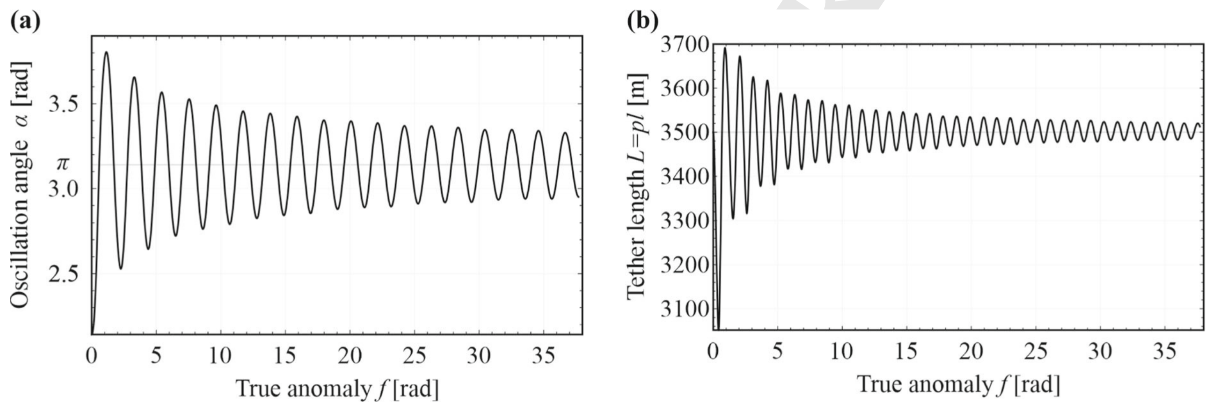

Fig. 9 The deployment of the tether toward Mars. **a** The oscillation angle α, **b** the tether length $L = p\,l$

– the deployment of the tether toward Phobos (Fig. 9), the control coefficient $\lambda = -4 \cdot 10^{-5}$.

At the end of the first stage, suppose that the tether oscillation amplitude α_m equals to 1 rad. Figures 8 and 9 illustrate the effectiveness of the control law (31), which provides damping of angular oscillations of the tether, while the tether remains stretched and the tension force does not exceed 0.1 N for the mass of the payload equal to 10 kg and for the initial deflection angle α_0 of the tether equal to 1.0 rad and for the initial ejection velocity V_0 = 2.0 m/s.

Figures 8 and 9 show that the angular stabilization of the tether requires much longer time than the main deployment of the tether, and the damping of tether oscillations occurs quite slowly, since according to the control law (31) as the deflection angle of the tether decreases, the control effect decreases. Although, on the other hand, it is shown in [27] that the control law (31) provides, on average, asymptotic stability.

5.4 Maintaining a constant distance from moon's surface

The stage of maintaining a constant distance to Phobos's surface using the control law (38) starts at the point in time when the primaries are at the perigee of the orbits. Numerical simulations are carried out with the following initial conditions

$$l_0 = 0.000377378, \quad l_0' = 0, \quad \alpha_0 = 0.1\,\text{rad}, \quad \alpha_0' = 0 \tag{41}$$

Figure 10 shows that at perigee, the tether length is 3580 m, at apogee, it is 4090 m (a), and during one orbital period of the primaries, the tether performs more than four complete oscillations (b), the amplitude of which varies insignificantly. Modeling in this

Journal : Medium 11071 Dispatch : 9-9-2021 Pages : 13
Article No. : 6884 ☐ LE ☐ TYPESET
MS Code : NODY-D-21-00862R1 ☑ CP ☑ DISK

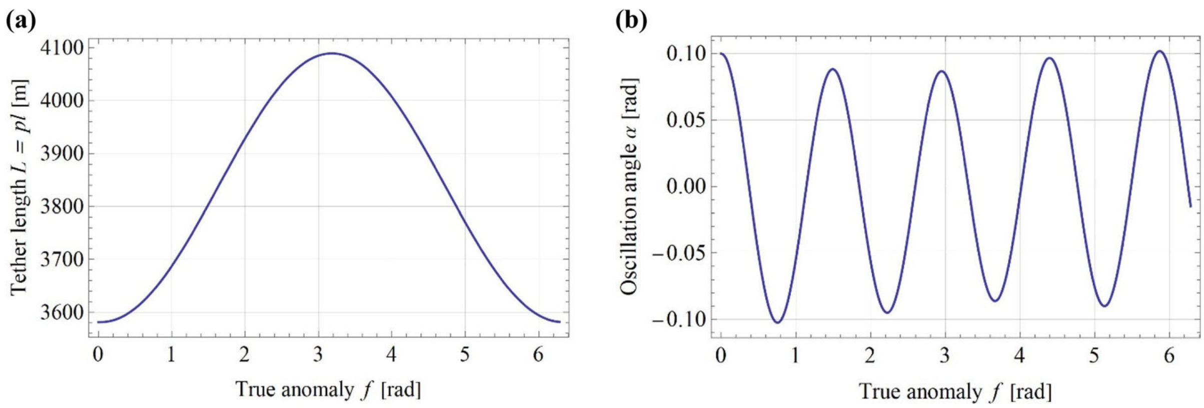

Fig. 10 **a** The tether length $L = p\,l$, **b** the oscillation angle α

case indicates that the tether remains always stretched and the tension force does not exceed 0.025 N for the mass of the payload is equal 10 kg.

Thus, the numerical simulations have shown the effectiveness of the proposed control laws of the tether system at all stages of the mission for the Mars-Phobos system.

6 Conclusions

The main results and conclusions about the applicability of the proposed mission architecture, mathematical models and control laws can be summarized as follows:

1. The deployment in three consecutive stages (main deployment, angular stabilization, and maintaining a constant distance to moon's surface) has been substantiated and verified by numerical simulations.
2. The motion equation for a weightless and inextensible tether with an end mass. The energy integral of the equation and the period of tether oscillation relative to the stable equilibrium positions have been found. It has been shown that the tether can rotate or oscillate relative to the two positions of stable equilibrium, which lie on the line connecting the primaries. In addition, it has been noted that in gravitational fields of two heavy bodies in a rotating frame, the oscillation frequency of the pendulum "attached" to the point L1 increases with increase in the length, in contrast to classical mathematical pendulum, in which the frequency decreases with increasing the length of the pendulum.
3. The proposed control laws of the tether tension force satisfy the requirements of the each stage as shown by numerical simulations, and these control laws are characterized by simplicity.
4. The tether deployment mission scene consisting of three consecutive phases proposed in the paper is not the only possible scene. Alternative schemas are quite possible and this may be the subject of the following works.

These studies confirm the feasibility of the PHLOTE mission and provide some theoretical justification for the mission. In all likelihood, this is the first analytical study of the motion of a tether system in the two-body gravitational field in terms of the restricted elliptic three-body problem, which complements both the three-body problem and the tether space systems problem.

In continuation of this study, we can consider motion of the tether system, taking into account motion of an orbiter in a small vicinity of the libration point. In addition, the proposed approach may be useful as other planet-moon systems and for other collinear libration points, for example L2 libration point.

Acknowledgements This study was supported by the Russian Science Foundation (Project No. 19-19-00085).

Data availability statement The datasets generated during and/or analyzed during the current study are available from the corresponding author on reasonable request.

Journal : **Medium 11071** | Dispatch : **9-9-2021** | Pages : **13**
Article No. : **6884** | ☐ LE | ☐ TYPESET
MS Code : **NODY-D-21-00862R1** | ✔ CP | ✔ DISK

Declarations

Conflict of interest The author declares that he has no conflict of interest.

References

1. Beletsky, V.V., Levin, E.V.: Dynamics of Space Tether Systems. Univelt Incorporated, San Diego (1993)
2. Levin, E.M.: Dynamic Analysis of Space Tether Missions. Univelt Incorporated, San Diego (2007)
3. Troger, H., Alpatov, A.P., Beletsky, V.V., Dranovskii, V.I., Khoroshilov, V.S., Pirozhenko, A.V., Zakrzhevskii, A.E.: Dynamics of Tethered Space Systems. CRC Press, New York (2010)
4. Aslanov, V.S., Ledkov, A.S.: Dynamics of Tethered Satellite Systems. Woodhead Publishing, Cambridge (2012)
5. Williams, P., Hyslop, A., Stelzer, M., Kruijff, M.: YES2 optimal trajectories in presence of eccentricity and aerodynamic drag. Acta Astronaut. **64**(7), 745–769 (2009). https://doi.org/10.1016/j.actaastro.2008.11.007
6. Williams, P., Blanksby, C., Trivailo, P.: Tethered planetary capture maneuvers. J. Spacecr. Rocket. **41**(4), 603–613 (2004). https://doi.org/10.2514/1.1024
7. Jung, W., Mazzoleni, A.P., Chung, J.: Nonlinear dynamic analysis of a three-body tethered satellite system with deployment/retrieval. Nonlinear Dyn **82**, 1127–1144 (2015). https://doi.org/10.1007/s11071-015-2221-z
8. Huang, P., Zhang, F., Chen, L., et al.: A review of space tether in new applications. Nonlinear Dyn **94**, 1–19 (2018). https://doi.org/10.1007/s11071-018-4389-5
9. Yu, B.S., Xu, S.D., Jin, D.P.: Chaos in a tethered satellite system induced by atmospheric drag and Earth's oblateness. Nonlinear Dyn **101**, 1233–1244 (2020). https://doi.org/10.1007/s11071-020-05844-8
10. Ledkov, A., Aslanov, V.: Evolution of space tethered system's orbit during space debris towing taking into account the atmosphere influence. Nonlinear Dyn **96**, 2211–2223 (2019). https://doi.org/10.1007/s11071-019-04918-6
11. Kumar, K.D., Kumar, K.: Attitude maneuver of dual tethered satellite platforms through tether offset change. J. Spacecr. Rocket. **38**(2), 237–242 (2001). https://doi.org/10.2514/2.3676
12. Kumar, K., Yasaka, T.: Rotation formation flying of three satellites using tethers. J. Spacecr. Rocket. **41**(6), 973–985 (2004). https://doi.org/10.2514/1.14251
13. Cartmell, M.P., McKenzie, D.J.: A review of space tether research. Prog. Aerosp. Sci. **44**(1), 1–21 (2008). https://doi.org/10.1016/j.paerosci.2007.08.002
14. Mashayekhi, M.J., Misra, A.K.: Optimization of tether-assisted asteroid deflection. J. Guid. Control. Dyn. **37**(3), 898–906 (2014). https://doi.org/10.2514/1.60176
15. Aslanov, V.S., Ledkov, A.S., Misra, A.K., Guerman, A.D.: Dynamics of space elevator after tether rupture. J. Guid. Control. Dyn. **36**(4), 986–992 (2013). https://doi.org/10.2514/1.59378
16. Kempton, K., Pearson, J., Levin, E., Carroll, J., Amzajerdian, F.: Phase 1 Study for the Phobos L1 Operational Tether Experiment (PHLOTE). End Report, NASA, pp.1–91. https://ntrs.nasa.gov/search.jsp?R=20190000916 (2018).
17. Sun, G., Zhu, Z.: Fractional-order tension control law for deployment of space tether system. J. Guid. Control. Dyn. **37**(6), 2057–2167 (2014). https://doi.org/10.2514/1.G000496
18. Yu, B., Jin, D., Wen, H.: Nonlinear dynamics of flexible tethered satellite system subject to space environment. Appl. Math. Mech. Engl. Ed. **37**, 485–500 (2016). https://doi.org/10.1007/s10483-016-2049-9
19. Szebehely, V.: The Restricted Problem of Three Bodies. Academic Press Inc., New York (1967)
20. Luo, T., Pucacco, G., Xu, M.: Lissajous and halo orbits in the restricted three-body problem by normalization method. Nonlinear Dyn **101**, 2629–2644 (2020). https://doi.org/10.1007/s11071-020-05875-1 AQ4
21. Zotos, E.E.: Classifying orbits in the restricted three-body problem. Nonlinear Dyn **82**, 1233–1250 (2015). https://doi.org/10.1007/s11071-015-2229-4
22. Ferrari, F., Lavagna, M.: Periodic motion around libration points in the elliptic restricted three-body problem. Nonlinear Dyn **93**, 453–462 (2018). https://doi.org/10.1007/s11071-018-4203-4
23. Woo, P., Misra, A.K.: Equilibrium points in the full three-body problem. Acta Astronaut. **99**, 158–165 (2014). https://doi.org/10.1016/j.actaastro.2014.02.019
24. Biggs, J.D., Negri, A.: Orbit-attitude control in a circular restricted three-body problem using distributed reflectivity devices. J. Guid. Control. Dyn. **42**(12), 2712–2721 (2019). https://doi.org/10.2514/1.G004493
25. Alessi, E.M., Sánchez, J.P.: Semi-analytical approach for distant encounters in the spatial circular restricted three-body problem. J. Guid. Control. Dyn. **39**(2), 351–359 (2016). https://doi.org/10.2514/1.G001237
26. Markeev, A.P.: Libration Points in Celestial Mechanics and Astrodynamics. Nauka, Moscow (1978).. (**in Russian**)
27. Aslanov, V.S.: Stability of a pendulum with a moving mass: the averaging method. J. Sound Vib. **445**, 261–269 (2019). https://doi.org/10.1016/j.jsv.2019.01.021

Publisher's Note Springer Nature remains neutral with regard to jurisdictional claims in published maps and institutional affiliations.

Journal : Medium 11071 | Dispatch : 9-9-2021 | Pages : 13
Article No. : 6884 | ☐ LE | ☐ TYPESET
MS Code : NODY-D-21-00862R1 | ☑ CP | ☑ DISK

Journal : **11071**
Article : **6884**

Author Query Form

Please ensure you fill out your response to the queries raised below and return this form along with your corrections

Dear Author

During the process of typesetting your article, the following queries have arisen. Please check your typeset proof carefully against the queries listed below and mark the necessary changes either directly on the proof/online grid or in the 'Author's response' area provided below

Query	Details Required	Author's Response
AQ1	Kindly check and confirm the street information is correct for affiliation.	
AQ2	Please check whether the intended meaning of the sentence 'The classical equations in … their mass center' is clearly conveyed.	
AQ3	As per the information provided by the publisher, Fig. 6 will be black and white in print; hence, please confirm whether we can add "colour figure online" to the caption.	
AQ4	As References [20] and [21] are same, we have deleted the duplicate reference and renumbered accordingly. Please check and confirm.	